

RSC Advances



This is an *Accepted Manuscript*, which has been through the Royal Society of Chemistry peer review process and has been accepted for publication.

Accepted Manuscripts are published online shortly after acceptance, before technical editing, formatting and proof reading. Using this free service, authors can make their results available to the community, in citable form, before we publish the edited article. This *Accepted Manuscript* will be replaced by the edited, formatted and paginated article as soon as this is available.

You can find more information about *Accepted Manuscripts* in the [Information for Authors](#).

Please note that technical editing may introduce minor changes to the text and/or graphics, which may alter content. The journal's standard [Terms & Conditions](#) and the [Ethical guidelines](#) still apply. In no event shall the Royal Society of Chemistry be held responsible for any errors or omissions in this *Accepted Manuscript* or any consequences arising from the use of any information it contains.

Cite this: DOI: 10.1039/c0xx00000x

www.rsc.org/xxxxxx

ARTICLE TYPE

Micellar charge induced emissive response of a bio-active 3-pyrazolyl-2-pyrazoline derivative: A Spectroscopic and Quantum Chemical analysis

Arindam Sarkar^a, Soumyadipta Rakshit^a, Sayantani Chall^a, Soumya Sundar Mati^a, Dipti Singharoy^a, Jorge Bañuelos^b, Iñigo López Arbeloa^b and Subhash Chandra Bhattacharya^a

Received (in XXX, XXX) Xth XXXXXXXXX 20XX, Accepted Xth XXXXXXXXX 20XX

DOI: 10.1039/b000000x

The *medium charge* specific excited state behaviour of a bio-active and fluorescent 3-pyrazolyl-2-pyrazoline derivative (PYZ) were systematically monitored in aqueous solutions of ionic (CTAB, SDS) and non-ionic (Triton X-100) micelles, applying steady state and time resolved fluorescence spectroscopy in addition to theoretical molecular simulations. PYZ displays complementary emission characteristics according to the nature of effective charge of the micelles which was rationalized on the very fundamental basis of frontier molecular orbital approach as obtained from quantum chemical calculations involving Time Dependent Density Functional Theory (TD-DFT) in combination with B3LYP exchange correlation function using 6-31G(d, p) as basis set. Dynamic Light Scattering (DLS) measurements provided crucial information regarding the fluorescence quenching pattern of micelle bound PYZ by quencher CpCl. This study essentially accentuate on PYZ's photophysical response in different micellar medium in conjunction with their individual mode of *electrostatic* interaction therein. The theoretically calculated HOMO-LUMO energy gap values provide adequate information about the emissive behaviour of PYZ in ionic micellar media. The variation in the lifetime values of PYZ in aqueous and micellar media act as an added evidence to the fact that PYZ basically reside in different micro-environments as introduced by the respective micelles. Conclusively it was observed that, in the excited state, PYZ responded promptly and uniquely according to the nature of *micellar charge*.

Introduction

Electrostatic interactions play a crucial role in modulating and stabilizing molecular interactions in organized assemblies and membrane-mimetic systems such as micelles¹. The electrostatic interfacial potential generated at the membrane-solution interface (arising from the membrane charge) plays a pivotal role in a variety of membrane-associated phenomena like ion binding and transport, ligand recognition etc². Micelles formed by ionic and non-ionic surfactants simulate a more complex environmental condition present in larger bio-aggregates. As a consequence, reactions occurring within micellar media gain tremendous importance due to their micro-environmental similarity with proteins, enzymes and their vivid membrane-mimicking nature. The most significant property of "micelles" is their ability to stabilize and bind solute molecules that are typically insoluble or sparingly soluble in pure bulk solvent³⁻⁶. In other words they act as efficient binders and carriers for targeted drug-delivery⁷⁻¹⁰. They are also extensively used in the aqueous-phase catalysis to improve the reaction rate owing to the solubilisation effects and supplying large reaction interfaces¹¹⁻¹⁴. The ionic micelle consists of a micelle-water interface which can be modulated by the embodiment of sensor molecules or ions¹⁵⁻¹⁸. Among the various physical methods used to monitor such micellar media,

photophysical methods based on fluorescence spectroscopy stand out due to their simplicity, wide scope and extreme sensitivity^{19, 20}. With the introduction of a properly selected environment sensitive fluorophore; one can follow the process of micellization and the effect of interfacial electrical field on its spectroscopic behaviour. 3-pyrazolyl-2-Pyrazoline derivatives constitute such a class of fluorescent probes possessing profound pharmaceutical and biological importance. Recent trend to synthesize these types of fluorophores has noticeably increased due to their anti-inflammatory, antidiabetic, anaesthetic, analgesic and glutamate transport sensing properties²¹⁻²⁵. They stand out due to their simple structure, large extinction coefficient, high quantum yields (0.6–0.8) and profound medium sensitivity^{26, 27}. Earlier works from our research group revealed that the ground and excited state behaviours of 2-pyrazoline derivatives are significantly influenced by the surrounding medium²⁸⁻³³. We herein report the photophysical response of a newly synthesized pyrazoline derivative (PYZ) in cationic CTAB, anionic SDS and non-ionic Triton X-100 (TX-100) micelles applying relevant spectroscopic techniques and various quantum chemical calculations. The ionic micelles were chosen with an aim to observe the effect of varying micellar interfacial charge on the conformation and dynamics of

micelle-bound PYZ. The compound has phenyl group at N(1) position of pyrazoline with methyl and cyano substitution at C(3) and C(4) position of pyrazole, respectively (*Scheme 1a*). The phenyl substitution at N(1) position of pyrazoline ring makes it highly fluorescent and the extended conjugation from 2-pyrazoline to pyrazole ring enhances the fluorescence intensity of the compound. The presence of cyano group C(4) makes it a potential hydrogen bonding site, due to the polarity difference of the C-N bond. The dipole moment of PYZ is expected to be greater in the excited state (S_1), owing to the greater charge separation than in the ground state (S_0) and also because excitation of PYZ increases its dipole moment³². The difference in micellar charge initiates a different type of interaction of PYZ with ionic micelles (CTAB and SDS) than with non-ionic TX-100 micelles. This was experimentally monitored by steady state emission study and CpCl induced fluorescence quenching studies of the excited PYZ molecule in all of the aforesaid micellar media. Time resolved fluorescence results provided a fruitful insight about the probable distribution of PYZ within each micellar medium of specific charge and polarity. To provide further evidence in support of the experimental spectroscopic parameters, quantum chemical calculations were carried out for free PYZ and PYZ-micelle systems. Electronic transitions were simulated by the Time Dependent Density Functional Theory (TD-DFT) method in combination with B3LYP exchange correlation function and 6-31G(d,p) as basis set. The HOMO-LUMO energy gap values (from TD-DFT calculations) of free and micelle bound PYZ provided necessary information regarding PYZ-micelle interaction. The theoretically calculated HOMO-LUMO energy gap values of the probe-micelle systems suitably exemplified PYZ's charge specific spectral response.

2. Materials and Methods

2.1. Reagents and Materials

PYZ ($C_{32}H_{24}N_3Br$; MW: 556) [5-((4'S, 5'R)-1'-(4-Bromophenyl)-4',5'-dihydro-4',5'-diphenyl)-1H-pyrazol-3-yl)-3-methyl-1-phenyl-1H-pyrazole-4-carbonitrile] was synthesized following procedure as described³⁴. Anionic surfactant SDS (Sodium Dodecyl Sulphate) was purchased from BDH; cationic surfactant CTAB (Cetyl Trimethyl Ammonium Bromide), nonionic surfactant TX-100 (Triton X-100) and quencher CpCl (Cetyl Pyridinium Chloride) were procured from Aldrich and were used as received. Triply distilled water was used for the preparation of all the experimental solutions. All the experiments were carried out at 298 K and at neutral pH (aqueous) medium.

2.2. Instrumentation:

2.2.1. Absorption Measurements: Absorption spectra were recorded using a Shimadzu UV-Vis 1700 spectrophotometer with a matched pair of silica cuvettes of path length 1 cm.

2.2.2. Steady state emission measurements: Fluorescence spectra were taken in an F-IIA Spectrofluorometer (Spex, Inc. NJ, USA) with an external slit width of 1.25 nm. All the measurements were reproducible.

2.2.3. Time resolved Fluorescence decay: Fluorescence lifetimes were determined from time-resolved fluorescence decay by the method of time-correlated single-photon counting (TCSPC) using

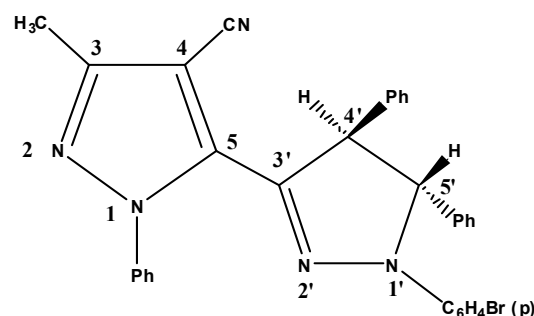
a nanosecond diode laser at 370 nm (IBH, picoLED-07) as light source with response time 1.1 ns. The obtained fluorescence decay curves were analyzed by the bi-exponential iterative fitting decay analysis software IBH DAS-6. Average lifetimes for all the bi-exponential decays were calculated from the fluorescence decay curves using the following equation⁴³.

$$\langle \tau_i \rangle = \frac{\alpha_1 \tau_1 + \alpha_2 \tau_2}{\alpha_1 + \alpha_2}$$

Here, α_i is a pre-exponential factor representing the fractional contribution of the decaying component with a lifetime τ_i .

2.2.4. Dynamic Light scattering studies: Dynamic Light Scattering (DLS) measurements were performed using a Nano-ZS 90-Malvern instrument (Model DLS-nano ZS, Zetasizer, Nano series) employing a 4 mW He-Ne laser ($\lambda = 632.8$ nm) equipped with a thermostatic sample chamber. All measurements were taken at 173° scattering angle and at 298 K. Size distribution of the samples were calculated using the associated instrument software. Samples were filtered thoroughly through a 0.2 μ m Millipore membrane filter prior to measurements to avoid possible presence of any dust particle.

2.2.5. Theoretical Quantum Chemical simulations: All energy calculations and electronic transitions of PYZ (in micelles/micelles-quencher media) were simulated by the Time Dependent Density Functional Theory (TD-DFT) method in the windows version of **Gaussian-09^{HR}** software package. The hybrid **B3LYP** exchange correlation function along with basis set **6-31G(d,p)** were adopted for all TD-DFT calculations. At first, the molecules were geometrically optimized (energy minimization) in their respective *ground states* (S_0) followed by excited state energy calculations in their *first singly excited states* (S_1). The ground state geometrically optimized structures corresponded to the true minima of the potential energy surface when the frequency analysis did not give any negative values. This was verified from *vibrational* frequency calculations³⁵. All TD-DFT calculations were carried out by selecting water as the solvent medium using Tomasi's³⁶ Polarized Continuum Model (PCM).



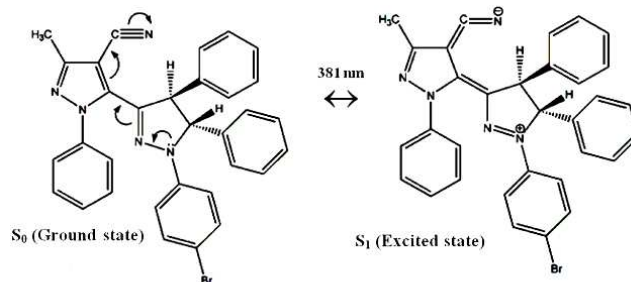
Scheme 1a: 5-((4'S, 5'R)-1'-(4-Bromophenyl)-4',5'-dihydro-4',5'-diphenyl)-1H-pyrazol-3-yl)-3-methyl-1-phenyl-1H-pyrazole-4-carbonitrile [PYZ]

3. Results and Discussions

3.1. Absorption and Steady State Emission:

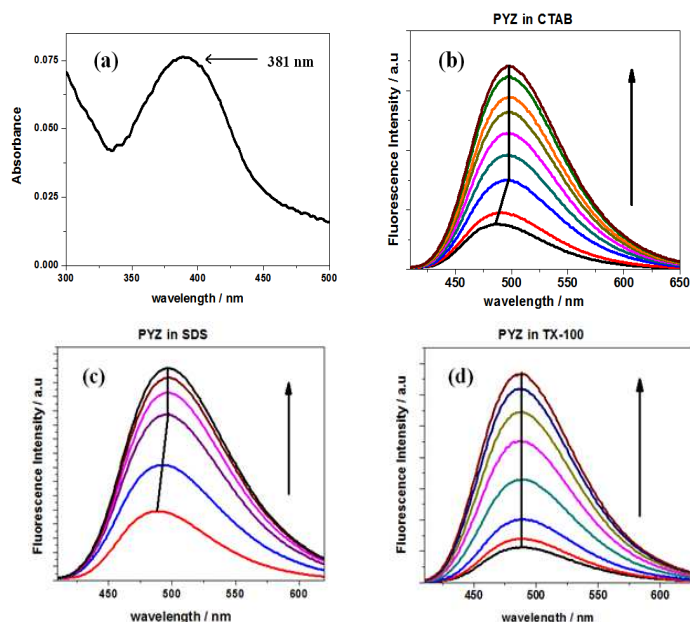
The absorption spectrum of an aqueous solution of PYZ produces a well resolved band with maxima at around 381 nm due to a $\pi \rightarrow \pi^*$ transition to the S_1 state (Figure 1a). When compared to an aqueous media³², the environment produced by the micelles does not cause any significant alteration in the absorption spectrum of PYZ. However, in contrast to the insensitive nature of absorption maximum of PYZ, the fluorescence spectra of PYZ are significantly affected in all the micellar media. The effect of micelles (CTAB, SDS and TX-100) on the fluorescence spectra of PYZ has been illustrated in Figure 1(b, c & d) respectively. An aqueous solution of PYZ exhibits fluorescence maximum at 485 nm. With a fixed concentration of PYZ in aqueous solution, the fluorescence intensities of PYZ increased steadily with increasing surfactant concentration (CTAB, SDS and TX-100). Gradual addition of CTAB and SDS solutions also stimulated a significant red shift (≈ 14 nm) in the fluorescence wavelength maxima of PYZ. The change in emission maxima of PYZ occurs around the cmc of the ionic surfactants (CTAB & SDS). The prominent red shift in the emission maxima of PYZ in ionic micelles can be explained by the electrostatic nature of interaction between PYZ and the ionic micelles. However, the red shift in PYZ emission maxima at surfactant concentration lower than its cmc possibly occurs due to the formation of pre-micellar aggregates of the ionic surfactants in the solutions besides charged electrostatic interactions between PYZ and the ionic monomers of CTAB and SDS. The charged CN^- and $N-2^+$ centers of PYZ predominantly interacts with the hydrophilic ionic parts (NH_4^+ & SO_4^{2-}) of CTAB & SDS respectively which appreciably shifts the PYZ emission maxima to a longer wavelength. After cmc, there is no further shift in PYZ emission maxima other than an increase in its fluorescence intensity. After reaching a certain concentration of the surfactants, PYZ's fluorescence intensity remained unaltered (corresponding to a fully micellized state of PYZ). Also the transition in shape and mode of aggregation of CTAB and SDS (surfactant \rightarrow micelles) is another probable reason for inducing a noticeable change in the spectral response of PYZ; since the shift in emission maxima of PYZ primarily occurs near the cmc of the ionic surfactants. However, in non-ionic TX-100, no shift in emission maxima of PYZ was observed as compared to that in CTAB and SDS. The emission intensity of PYZ enhanced significantly with addition of TX-100 (both in pre-micellar and micellar region) but without any perturbation in the wavelength maxima. The red-shifted fluorescence maxima exhibited by PYZ in ionic micellar media (CTAB and SDS) is comparable to that of the emission maxima of PYZ in polar homogeneous media and solvents possessing hydrogen bond formation capability³². This generally indicates that PYZ experiences a polar micro-environment in the micelles of CTAB and SDS but this assumption can be ruled out because a micellar media is always less polar than bulk aqueous medium. In one of our earlier works another derivative PZ exhibited blue shift in micellar media of CTAB and SDS³⁰. So, a blue-shift is generally expected to occur under such conditions. Since PYZ displayed a prominent red shift in ionic micellar media, hence; the most possible scenario would be that PYZ is primarily solubilized at the micellar

interfacial site where they can interact with the surfactant head groups and can also be solvated partially by the surrounding bulk water molecules. PYZ interacts with polar-protic solvents via hydrogen bonding through the lone pair of electrons on the $-CN$ group of PYZ with that of the $-OH$ group of the polar-protic solvent molecule³². The increase in dipole moment of PYZ makes it more facile for interaction in the excited state. This uncharacteristic spectral response of PYZ in CTAB and SDS micelles is definitely caused by the specific probe-micelle



Scheme 1b: Excitation mechanism PYZ

interactions occurring between the polar head groups or counter ions of the micelles and the polar substituent's (N and Br) in PYZ. The red-shift in the emission maxima of PYZ also arises due to the involvement of polar and conformationally-relaxed electron transfer states, whose stability is significantly influenced



by changing the micro-polarity of the micellar medium.

Figure 1: (a) Absorption spectra of PYZ in water. Emission profile of PYZ in (b) CTAB (c) SDS and (d) TX-100; [PYZ] = 6.8×10^{-6} M in all sets; (b) [CTAB] = 0 to 4.7 mM; (c) [SDS] = 0 to 28.7 mM and (d) [TX-100] = 0 to 2.5 mM; $\lambda_{\text{exc}} = 381$ nm

Conversely, the emission profile of PYZ in TX-100 basically generates from the locally excited planar state. PYZ is apparently located in a more hydrophobic TX-100 micro-environment since specific ionic interaction between PYZ and non-ionic TX-100 is not possible. The constrained TX-100 micellar network inhibits conformational motions within bulky PYZ molecule, thereby

diminishing the polarity of the excited state. As a result, PYZ fluoresce at almost the same wavelength in TX-100 as it does in bulk aqueous medium. The rigidity of the alkyl chains of CTAB, SDS, and the hydrophobicity of TX-100 micelles hinders all other molecular motions and non-radiative transitions occurring within PYZ, thus resulting in an overall increase in the PYZ fluorescence intensity. PYZ interacts efficiently with ionic CTAB and SDS in the excited state via electrostatic interactions through the oppositely charged centers ($[-CN^-]$ and $[N-2^+]$) respectively; (Scheme 1b) resulting in the formation of a highly emissive and stable (low energy & long wavelength) PYZ-micelle assembly.

3.1.1. PYZ-Micelle Binding:

Micelles are essentially characterized by two regions, a hydrophobic core and a hydrophilic surface that may be cationic, anionic and non-ionic. All these three types of micelles consist of a dry hydrocarbon core surrounded by a wet spherical shell called the Stern layer with thickness 6–10 Å for ionic micelle and 25 Å for palisade layer of non-ionic micelle. Surrounding the Stern layer is a diffuse layer called the Gouy Chapman layer. This outer layer is about several hundred angstroms wide^{15, 18}. The enhancement in fluorescence intensity of PYZ in both (ionic and nonionic) micellar media can be rationalized in terms of binding of the probe with the micelles. The strength of the binding can be identified through the determination of the binding constant K of the probe with the micelles. The binding constants between the probe and the micelles have been determined from the fluorescence intensity data following the method described by Almogren et al.³⁷ and the binding constant values so obtained are given in Table 1. According to the equation:

$$\frac{(F_m - F_0)}{(F - F_0)} = 1 + (1 / K [M]) \dots \dots \dots (1)$$

Where, F_0 , F , and F_m are the fluorescence intensities of PYZ in absence of surfactant, in presence of micelles (micellar concentration $[M]$), and at maximum micellar concentration respectively. K represents the binding constant between the probe in the excited state and micelle. The micellar concentration $[M]$ has been calculated using the surfactant concentration $[S]$ as $[M] = ([S] - CMC) / n$, where n is the aggregation number of the surfactant^{38, 39}. The plot of $[(F_m - F_0) / (F - F_0)]$ vs $(1/[M])$ (from equation 1) produced a well fitted linear plot (Figure S1). From the slopes of the individual plots, the binding constants (K) (Table 1) have been determined. The K values indicate that PYZ binds strongly with TX-100, CTAB and SDS and they follow the order TX-100 > SDS > CTAB. Three distinct regions are observed in a micelle, a nonpolar core formed by the hydrocarbon tail of the surfactant, a compact Stern layer having the head groups or palisade layer for ionic and nonionic micelles respectively, and a wider Gouy–Chapman layer containing the counter ions. A probe molecule may bind either to the head-group region or to the nonpolar core of the micelles. Depending on the nature of the solute, the solute molecules may reside in any one of the sites. The Stern layer for ionic and palisade layer for nonionic micelles consists of polar head groups and largely structured water molecules. In nonionic micelle TX-100, the high binding constant of the probe is due to more stabilization of the probe in the TX-100 micellar medium compared to other ionic micelles. The size and hydrophobicity of TX-100 is appreciably

greater than either of CTAB and SDS. As a fact TX-100 provides more effective surface area for PYZ to bind steadily. Due to the very thick “Palisade layer” of the TX-100 micelles, PYZ molecules primarily reside in this layer where the water structure is not as loose as that in the “Stern layer” of CTAB and SDS micelles which have significantly thinner micellar radii than the palisade layer of TX-100. PYZ also experiences a greater microviscosity in the palisade layer of TX-100 due to a greater extent of packing of the surfactant chain⁴⁰. Between the two ionic micelles CTAB and SDS, despite the comparable thickness of the Stern layer; binding constant of PYZ with SDS is higher than that with CTAB. Although the mode of binding essentially seems to arise from strong hydrophobic interaction between the hydrophobic tail of CTAB and bulky PYZ molecule, still the possibility of an electrostatic interaction between the positively charged quaternary ammonium head group and π -electron rich centers in PYZ cannot be ignored. The total binding is thus a combined effect of both the factors depending on their predominance. The formation of *pre-micellar* aggregates along with effective electrostatic interactions between PYZ and CTAB allows PYZ to emit at a longer wavelength (*more stable region*) thus producing a 14 nm red shift (*bathochromic*) of PYZ emission from bulk aqueous medium. Alike CTAB, the same trend was also observed in SDS, an anionic surfactant for which the binding is a combined factor arising due to both hydrophobic and electrostatic interactions. The electrostatic interaction has significantly increased the binding of SDS with PYZ as reflected from higher values of binding constant K in SDS. The binding constant of PYZ in SDS is consistently higher than that in CTAB which is a direct reflection of the fact that stronger electrostatic interaction persists between PYZ and SDS than with CTAB. The hydrophobic interactions between PYZ-micelle depend on the alkyl chain length of the surfactants. The longer alkyl chains of surfactants should exhibit more hydrophobic character than the shorter alkyl chains of surfactants. Considering the fact that the “net hydrophobicity” of an ionic surfactant depends on the number of carbons in the hydrophobic tail (n) and the total charge distribution in the surfactant, the “effective micellar charge” is least for the most hydrophobic compound (PYZ-CTAB; $n=16$) and highest for the least hydrophobic (PYZ-SDS; $n=12$). This shows that the electrostatic contribution towards the binding between PYZ and the ionic micelles decreases with increasing hydrophobic character of the micellar medium.

Table 1: Spectroscopic parameters of PYZ in aqueous and micellar media

PYZ medium	Emission maxima (λ_{max}^{fl})(nm)	(K) (mol ⁻¹ dm ³) x 10 ⁻³	(K _{SV})/(mol ⁻¹ dm ³) x 10 ⁻²	cmc (mol ⁻¹ dm ³) x 10 ³
Water	485	-----	-----	-----
CTAB	498	8.1	3.22	0.85
SDS	499	58.4	-----	8.18
TX-100	484	1662.1	17.2	0.24

Since electrostatic contribution is greater in SDS than in CTAB; hence the PYZ-SDS micellar assembly produces a higher binding constant value than the PYZ-CTAB system. The penetration of the probe depends on the nature/polarity of micellar core and varies in CTAB and SDS (CTAB has somewhat lower polarity than SDS). The aliphatic chain of CTAB is longer than that of SDS; thus the flexibility of the longer chain makes the movement of molecules easier towards the core of the micelles.

3.1.2. CpCl Induced Fluorescence Quenching:

To confirm the location of the fluorophore in the micellar media, fluorescence quenching studies of the probe were carried out in all the micellar media using CpCl as a quencher. In micellar media, fluorescence quenching is influenced by the distribution of fluorophores and quencher species in the micelles⁴¹. Here the quencher CpCl mixes ideally with the micelles⁴² and enters into the vicinity of “Stern layer” or “Palisade layer” where fluorescence quenching occurs essentially. Fluorescence quenching data are useful to rationalize the location of the fluorophore in the interfacial region or core of the micelle. The quenching pattern of the S₁ state of PYZ by the quencher CpCl in the micellar media, obtained from the steady state emission spectra are presented in Figure 2 (a, b, & c). A linear Stern-Volmer plot was obtained (Figure 2d), which can be described using the below equation⁴³

$$(F_0/F) = 1 + (K_{SV}[Q]) \dots\dots (2)$$

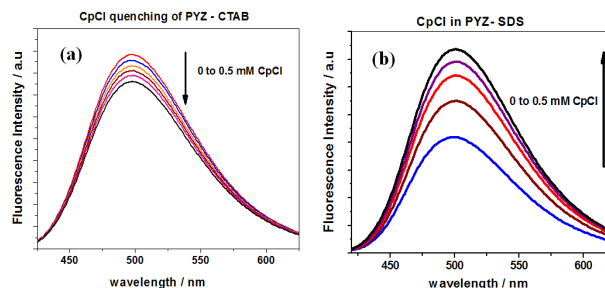
Where, F_0 and F represent the fluorescence intensities of micelle bound PYZ in absence and presence of quencher respectively. $[Q]$ represents the concentration of quencher and K_{SV} is the Stern-Volmer constant. The quencher is not supposed to be available in the micellar core because of the very low solubility in that region. It is expected to be available in the aqueous phase as well as in the micellar interfacial region. Hence; if the fluorophore is located in the micellar core, there should be no appreciable fluorescence quenching as a result of the lack of availability of the quencher near the fluorophore. However, because the probe is located at the micellar interfacial region then the CpCl induced quenching of the PYZ fluorescence occurs in micellar media. The quenching phenomenon is considered to be collisional where the rate of quenching is different in each micellar media due to difference in binding strengths of PYZ with the micelles. Appreciable fluorescence quenching of PYZ was observed in micellar media of TX-100 indicating the accessibility of the quencher CpCl to PYZ in the palisade layer of TX-100 micelles. A relatively low fluorescence quenching of PYZ occurred in cationic CTAB micelles which supports the fact that PYZ is not easily accessible to the quencher CpCl due to a different mode of interaction between PYZ and CTAB. Although PYZ presumably resides in the Stern layer of CTAB, yet CpCl is unable to quench it effectively thus indicating a different mode of interaction between PYZ and CTAB. It is assumed that due to electrostatic repulsion positively charged cetyl pyridinium ion is unable to approach the vicinity of the “Stern region” of cationic CTAB micelles where PYZ resides predominantly. However, appreciable quenching has been observed in this same system (CTAB-CpCl) using other PYZ derivative³⁰. This ignites the idea that a different type of interaction certainly persists between PYZ

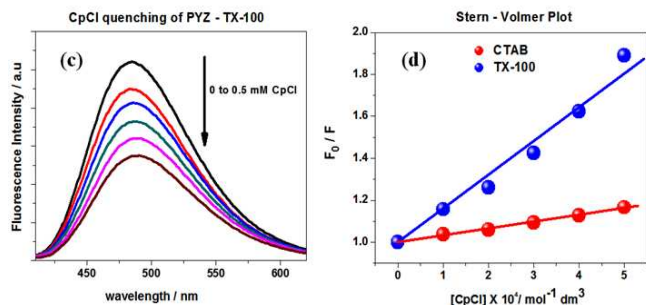
and CTAB thereby causing relatively low fluorescence quenching by CpCl. Hence, contrary to the normal expectation of quenching of the fluorescence of PYZ by the said ion, the quencher cannot come closer and communicate to the fluorophore efficiently, and as a result, we observe only an insignificant quenching of the fluorescence of PYZ in CTAB.

3.1.3. Anomalous Enhancement of emission of SDS bound PYZ on CpCl addition:

Surprisingly, the quenching study of PYZ in SDS yielded totally opposite results. With addition of the quencher CpCl, the fluorescence intensity of PYZ increased significantly in anionic SDS micelles, which may be due to some specific interaction arising between the probe, the micelle and quencher (PYZ - SDS -CpCl), leading to the formation of an immediate microenvironment that facilitates an enhancement in the fluorescence intensity of PYZ. Earlier works show that CpCl interacts with SDS and forms vesicular aggregates but only when added in 1:1, 1:2 & 1:3 molar ratios. After achieving their solubility product, the SDS-CpCl solution forms vesicular aggregates or simply precipitates out⁴⁴. But here, these salts were taken at a concentration which is much less than their solubility product. So there isn't any formation of such vesicular aggregates. Also, the experimental solution didn't show any type of turbidity and was fully clear and transparent. A blank emission run was performed using only SDS-CpCl solution (without PYZ) in the desired spectral range (385 to 600 nm) where no spectra or curve was observed. Thus, the resulting emission intensity displayed by the PYZ-SDS-CpCl solution originated exclusively from PYZ only. But, instead of being quenched, the fluorescence intensity of PYZ enhanced appreciably in anionic SDS medium; with gradual addition of cationic quencher CpCl (up to 0.5 mM). The most apt explanation for this unique observation would be the rearrangement of the charged species (PYZ, SDS & CpCl) through specific dipolar interactions which increases the rigidity of the whole system. As a consequence, PYZ resides in a more rigid system, hence its interactions with bulk aqueous medium is reduced to a minimum. This leads to an enhancement in the emission intensity of PYZ which is why normal quenching of PYZ by CpCl does not occur at all.

Figure 2: CpCl induced fluorescence quenching of PYZ in (a) CTAB (b) SDS and (c) TX-100. $[CpCl] = 0$ to 0.5 mM in each set. $[PYZ] = 6.8 \times 10^{-6}$ M in all sets; $[CTAB] = 4.7$ mM; $[SDS] = 28.7$ mM; $[TX-100] = 2.5$ mM; $\lambda_{max}^{ex} = 381$ nm. (d) Stern-Volmer quenching plot of PYZ by quencher CpCl.





3.2. Dynamic Light scattering studies:

The effect of micellar chain length and the characteristic pore size of the micellar structures on the extent of incorporation of PYZ in all the micellar media were monitored implying dynamic light scattering measurements. Hydrodynamic diameters of the *micelles* and *micelle-quencher* systems were estimated from the intensity autocorrelation function of the time-dependent fluctuation in intensity. Hydrodynamic diameter is defined as

$$d_h = (k_b T) / (3\pi\eta D) \dots\dots(3)$$

Where, k_b is the Boltzmann constant, η is the solvent viscosity, and D is the translational diffusion coefficient.

In a typical size distribution graph from the DLS measurement, the X-axis shows a distribution of size classes in nanometers, whereas the Y-axis shows the relative intensity of the scattered light. The size of the micelles was determined using the DLS measurements. The hydrodynamic diameters obtained for *bare micellar* and *quencher-micellar* solutions follow the order TX-100 – CpCl > TX-100; CTAB – CpCl < CTAB and SDS – CpCl \approx SDS (Figure 3) which is direct evidence to the fact that CpCl was able to access the PYZ molecule and efficiently quench the PYZ emission inside the TX-100 micellar network, to the maximum extent. In CTAB, the quenching capacity of CpCl decreased significantly due to contraction in size from interaction between PYZ and CTAB whereas in SDS micellar medium it was unable to quench PYZ. It is observed that in aqueous and quencher medium, SDS micelles possess hydrodynamic diameter (d_h) \approx 1.5 nm indicating that the hydrodynamic diameter of the micelle remains unaltered upon addition with quencher CpCl. Given the fact that PYZ possesses dipolar character; it exhibit zwitter-ionic character and interacts with the head-group of the SDS micelle. Thus PYZ is expected to stay at the SDS micelle-water interface. Also, the CpCl-SDS system provided a more confined network to PYZ as a result of which the fluorescence intensity of PYZ increased dramatically in SDS after addition of

quencher CpCl. Further, the variation of the micro-viscosity of the SDS-CpCl system and change in micellar shape and arrangement of SDS in presence of CpCl^{45, 46} may be responsible for the augmented fluorescence intensity of PYZ in that particular *micelle-quencher* medium.

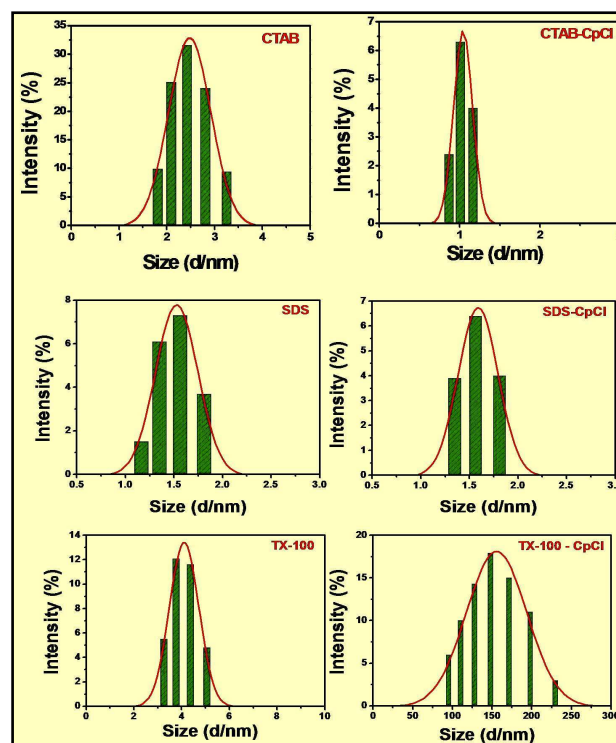


Figure 3: Dynamic Light Scattering (DLS) graph of CTAB, SDS and TX-100 with and without quencher CpCl; [CTAB] = 4.7 mM; [SDS] = 28.7 mM; [TX-100] = 2.5 mM; [CpCl] = 0.5 mM in each set.

3.3. Fluorescence Decay Measurements:

Fluorescence lifetime serves as a sensitive indicator of the local micro-environment in which a given fluorophore is placed⁴⁷. Lifetime based measurement provides rich information and unique insights into the systems under investigation^{48, 49}.

The emission decay profile of PYZ in aqueous micellar media were monitored using time-resolved study. The time constants for

Table 2: Fluorescence Decay parameters of PYZ in aqueous and micellar media

PYZ medium	A ₁	A ₂	τ_1 (ns)	τ_2 (ns)	τ_{avg} (ns)	χ^2
Water	0.92	0.08	1.11	4.17	1.35	1.12
SDS	0.72	0.28	1.18	4.05	1.98	1.16
CTAB	0.52	0.48	1.26	5.10	3.12	1.04
TX-100	0.30	0.70	1.04	6.05	4.55	1.18
SDS - CpCl	0.52	0.48	1.88	4.48	3.13	1.18
CTAB - CpCl	0.55	0.45	1.25	5.06	2.97	1.06
TX-100 - CpCl	0.43	0.57	1.75	4.50	3.32	1.14

fluorescence decays monitored at the emission band maxima are given in Table 2. In water, bi-exponential decay was observed (Figure 4a). All the other fluorescence decays for micelle bound PYZ were also fitted with a bi-exponential function. In heterogeneous micellar systems, a probe may exist in drastically different locations, e.g., the bulk water, hydrocarbon core of the micelles, and the micelle-water interface. The decay of the emission profile is thus expected to be multi-exponential. We assume that the multi-exponential nature of the decay curves of PYZ most likely arises due to reorientation of the probe molecule in two different microenvironments or their existence in more than one species in the micellar microenvironment.

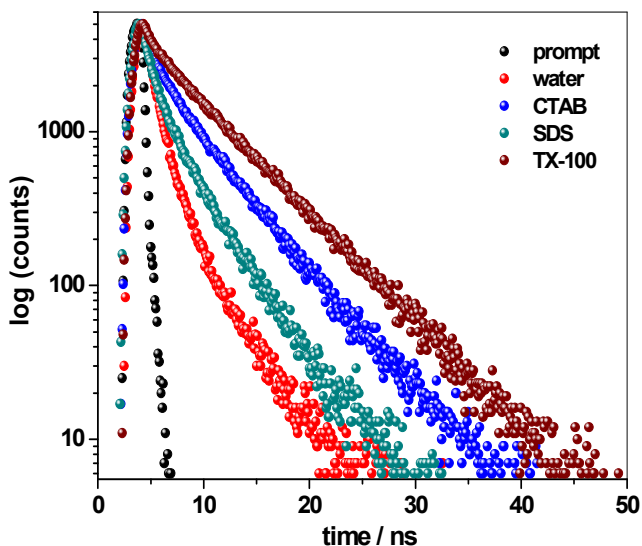


Figure 4: (a) Fluorescence Decay profile of PYZ in water, CTAB, SDS and TX-100. (b) Plot of distribution parameters of PYZ vs solvent dielectric constant; $\lambda_{\text{max}}^{\text{ex}} = 381 \text{ nm}$; $\lambda_{\text{max}}^{\text{em}} = 485 \text{ nm}$ (water); $\lambda_{\text{max}}^{\text{em}} = 498 \text{ nm}$ (CTAB); $\lambda_{\text{max}}^{\text{em}} = 499 \text{ nm}$ (SDS); $\lambda_{\text{max}}^{\text{em}} = 485 \text{ nm}$ (TX-100); $[\text{PYZ}] = 6.8 \times 10^{-6} \text{ M}$; $[\text{CTAB}] = 4.7 \text{ mM}$; $[\text{SDS}] = 28.7 \text{ mM}$; $[\text{TX-100}] = 2.5 \text{ mM}$.

The distribution width of both the forms varies considerably in water and other micellar media in conjunction with appreciable changes in the average lifetime values of PYZ. This qualitative change in the lifetime distribution profile is mainly caused by micelle-induced orientation modification of the PYZ local micro-environment. As observed from Table 2, PYZ shows a considerable increase in its average lifetime values in the order 'water < SDS < CTAB < TX-100'. The distribution parameter A_1 decreases accordingly from polar (water; 0.92) to non-polar (micellar; 0.30) medium. Conversely the A_2 values increases with decrease in medium polarity (0.08 in water to 0.70 in TX-100). To envisage the variation of A_1 and A_2 according to medium charge; the lifetime distribution parameters were plotted against micellar dielectric constant⁵⁰. Since dielectric constant directly reflects the effective charge of a particular medium, hence it was more reasonable to observe the variation of the PYZ decay parameters with the respective dielectric constants of the micelles. The obtained plot indicated a noticeable variation of the proposed PYZ species in different micellar media (Figure 4b). On the contrary, the predominance of (PYZ) in non-aqueous

(micellar) is reflected by the increasing A_2 values. A decrease in the average fluorescence lifetime of PYZ in SDS compared to CTAB micellar media may be due to the difference in nature and thickness of the Stern layer of CTAB and SDS which affects the mode and extent of binding of PYZ with those two micelles. In nonionic micelle TX-100, the lifetime of PYZ is higher compared to either of the ionic micelles. This can be ascribed to the additional stabilization of PYZ occurring due to its strong binding interaction with TX-100 owing to its relatively thicker Palisade layer than the Stern layer of the ionic micelles⁴⁰. Furthermore, fluorescence decays were also recorded for all three PYZ-micelle systems with added CpCl quencher in them. The obtained results were indeed very informative (Table 2). In CTAB bound PYZ, the lifetime of PYZ displayed a negligible decrease (0.15 ns) upon addition of quencher CpCl, indicating that the quencher was unable to appreciably quench the fluorescence of PYZ in CTAB micellar medium. Contrastingly, in SDS micellar medium, the lifetime of PYZ (3.1 ns) increased appreciably than its original value (2 ns), upon CpCl addition. This is a strong and direct evidence of the fact that PYZ truly experiences a completely different microenvironment within the SDS-CpCl system, which promptly increases its lifetime as opposed to the normal quenching pattern of a fluorophore. This also explains the enhancement of PYZ emission intensity in SDS micellar medium, when added with quencher CpCl. Our previous assumption, that unlike any normal fluorophore-micelle-quencher system, the arrangement PYZ-SDS-CpCl system provides a unique environment to PYZ which promptly increases its fluorescence intensity, is thus correctly and suitably justified from this lifetime measurement. In TX-100, lifetime of PYZ decreased prominently as expected (1.23 ns); implying that normal fluorescence quenching takes place in this case. This is too in accordance with the result obtained from fluorescence quenching study where the fluorescence intensity of PYZ in TX-100 was considerably quenched by CpCl.

3.4. Time Dependent Density Functional Theory (TD-DFT) calculations:

Frontier Molecular orbital's namely HOMO and LUMO play a vital role in determining the nature of a particular reaction where molecules interact with each other via electrostatic interactions. Density functional theory (DFT) has proven to be an important tool in modern quantum chemistry because of its ability to include some effects of electron correlation to build the electron density of a chemical system^{51, 52}. With the constructed density one can calculate a range of chemical properties of interest and a vivid picture of the frontier molecular orbitals namely HOMO and LUMO⁵³⁻⁵⁶. The TD-DFT/B3LYP/6-31G(d,p) calculations of PYZ-water and PYZ-micelle systems provided prominent and valuable insight concerning the photophysics of PYZ in each corresponding media. The molecule PYZ is typically characterized by a constrained geometry owing to the several phenyl rings in the pyrazol moiety. Such steric hindrance induce the two phenyl groups linked to the carbons of one pyrazol to be disposed perpendicularly, while the other one attached to the nitrogen has space enough to be coplanar with the pyrazol. However, in the other pyrazol bearing acetonitrile, the phenyl is twisted due to the proximity of the neighboring phenyl groups.

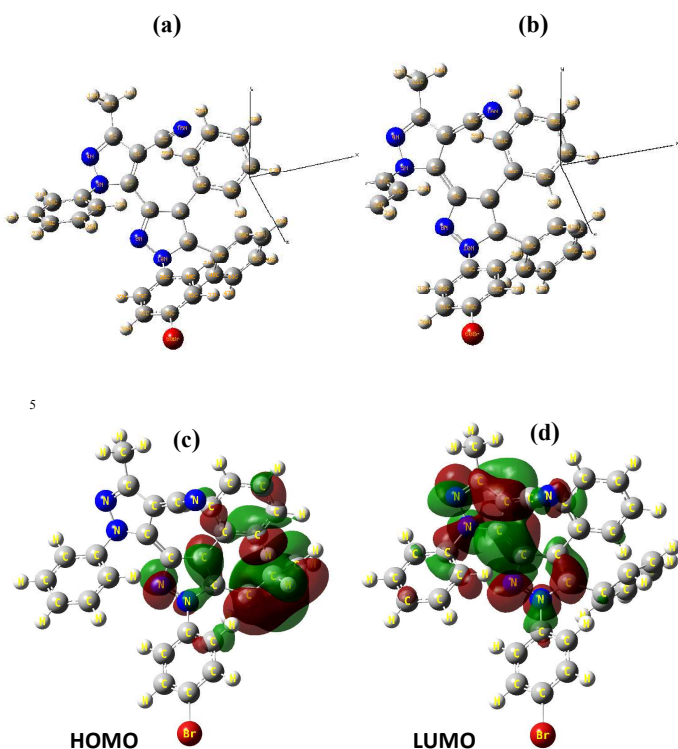


Figure 5: (a, b) Geometrically optimized structure of PYZ in its ground and excited states respectively. (c, d) TD-DFT/B3LYP/6-31G(d,p) computed excited state HOMO and LUMO diagrams of PYZ respectively.

Whereas these are common rules regardless of the solvent and the electronic state, the mutual orientation of the two pyrazols changes from the ground and excited state. While in the ground state these rings are twisted the excitation implies a more coplanar rotation. The PYZ thus can be described in terms of two proposed structures: the neutral PYZ molecule in the S_0 ground state and the zwitterionic PYZ* in the S_1 excited state. This essentially imply that the S_0 ground state corresponds mainly to the form PYZ, (Figure 5a) where the carbons connecting both rings are in an sp^3 hybridization, but the other form (PYZ*) (Figure 5b) prevails in the S_1 excited state, where the carbons are in sp^2 hybridized state. Upon excitation, the C(3') - C(5) bond length (linking the two pyrazol rings) decreases from 1.484 Å (S_0) to 1.381 Å (S_1), resulting in an increase in the resultant bond order. This clearly indicates a transition in the carbon hybridization state from sp^3 (single bond character) to sp^2 (double bond character). Even more, in the above optimized geometry, the calculation infers that delocalization occurs through such bond in the S_1 state but not in the S_0 state. The decreased value of C(3') - C(5) bond length of PYZ in the excited state is identified as a double bond, confirming that PYZ* exists in the excited state. This structure is characterized by a higher charge separation; therefore it is logical for it to be stabilized in polar media. In fact the dipole moment of PYZ in water increases upon excitation from 11.48 D to 12.82 D. Upon excitation, the negative charge on the nitrogen atom in -CN group increases due to

delocalization of a negative charge from PYZ to PYZ*.
 50 Considering this increase in the negative charge on -CN in the excited state, it is possible to analyze the interaction of PYZ in a particular micellar medium. Moreover, the stabilization of PYZ* in the respective micellar media results in an enhancement of its emission intensity, since the free rotation around the bond linking
 55 C(3') - C(5) (which changes from single to double) gets restricted due to the sp^2 character of the bonded carbon atoms. The simulation studies correctly predict that the electronic transition within PYZ is the result of promotion of one electron from the HOMO to the LUMO. This implies that, upon excitation of PYZ;
 60 transfer of an electron from one pyrazol to the other one bearing the electron withdrawing -CN group occurs promptly.

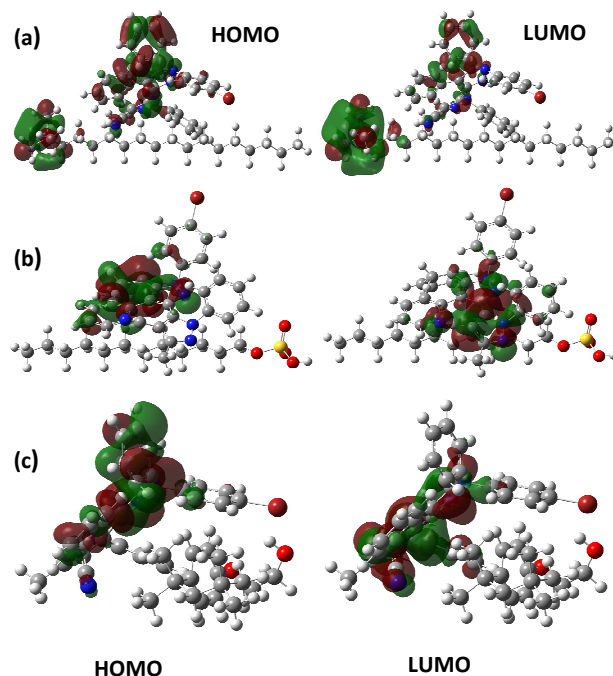


Figure 6: TD-DFT/B3LYP/6-31G(d,p) computed excited state HOMO and LUMO diagrams of (a) [PYZ-CTAB], (b) [PYZ-SDS] and (c) [PYZ-TX-100-CpCl] systems.

Figure 7: TD-DFT/B3LYP/6-31G(d,p) computed excited state HOMO and LUMO diagrams of (a, b) [PYZ-SDS-CpCl] & (c, d) [PYZ-TX-100-CpCl] systems respectively.

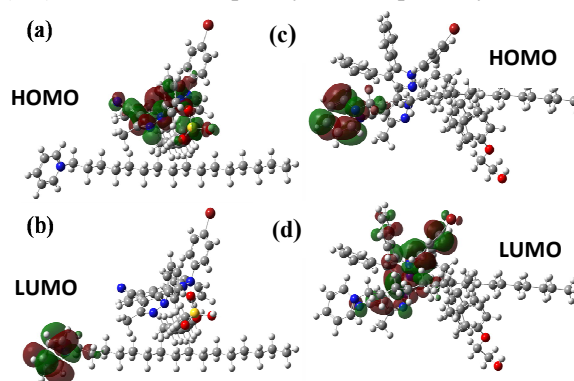


Table 3: Excited state HOMO, LUMO and Energy Gap of PYZ in micellar media using TD-DFT/B3LYP/6-31G(d,p)

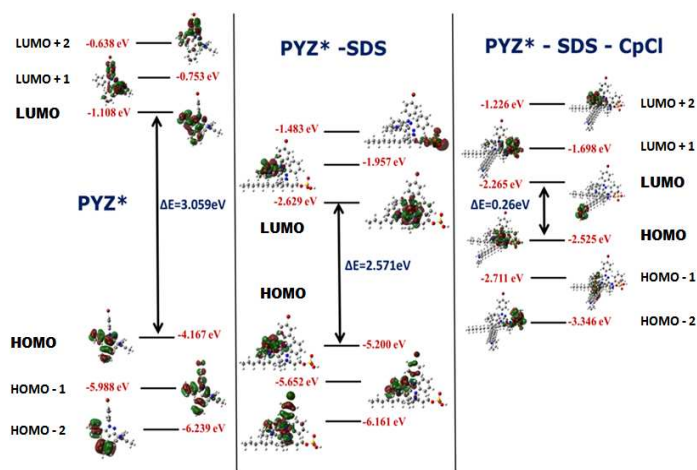
#System	HOMO (eV)	LUMO (eV)	ΔE (eV)
PYZ*	-4.167	-1.108	3.059
PYZ* – CTAB	-2.283	-0.633	1.650
PYZ* – SDS	-5.200	-2.629	2.571
PYZ* – SDS – CpCl	-2.525	-2.265	0.260
PYZ* – TX-100	-5.202	-2.526	2.676
PYZ* – TX-100 – CpCl	-5.497	-2.988	2.509

#Here PYZ indicates the Excited State (S_1) of PYZ*

The theoretically calculated contours of the HOMO and LUMO of optimized PYZ molecule in S_0 and S_1 states indicate that the HOMO's are predominantly delocalized over the whole PYZ molecule. On the other hand, the LUMO's are delocalized only through the acceptors and π -bridges (Figure 5c & 5d). Thus, when transition occurs from HOMO to LUMO by photo-excitation at 381 nm, the LUMO plays an important role in governing the resultant emission property of PYZ in a particular micellar medium. The contributions of HOMO LUMO orbitals for the highest absorption wavelength and the oscillator strengths were also verified (Figure S2). The energy difference between HOMO–LUMO is mainly caused by the perturbation of both the HOMO & the LUMO energy levels of PYZ. Molecules with large HOMO-LUMO gaps are generally stable and unreactive; while those with small gaps are generally reactive⁵⁷⁻⁵⁹. In one of their earlier works Zhang et.al⁶⁰ reported that the LUMO energy gets lowered when the LUMO is delocalized over more space. The emission properties, as well as the difference in HOMO–LUMO energy gaps of PYZ are affected in different ionic micellar media. Since excitation implies an important rearrangement in the electronic distribution of PYZ from S_0 to S_1 ; the transitions are characterized by a high electron transition probability (HOMO→LUMO). Considering that, in the S_1 state, the free motion of the bond linking both pyrazols is restricted, higher fluorescence capacities should be expected when such structure is stabilized by polar solvents (water) or through specific interactions (i.e., ionic surfactants like CTAB and SDS in this case). Depending on the degree of effective π -conjugation in it, PYZ displays variable HOMO–LUMO energy gaps in charged micellar media. Appreciable fluorescence enhancement associated with red-shift's in emission wavelength maxima were observed for PYZ in ionic micellar solutions (CTAB & SDS) indicating the occurrence of more effective π -conjugation in its S_1 excited state. The existence of two charged centers in PYZ* also facilitates in perturbing the MO energy levels of the probe in ionic micelles. The MO perturbation increases as the charge distribution in the whole system increases resulting in further variation of the HOMO-LUMO energy gaps. The lowering in HOMO-LUMO energy gap of PYZ ensured a high electron transition probability (HOMO→LUMO) in PYZ, thus allowing it to respond promptly by displaying a substantial increase in its emission intensity, as observed during its fluorescence study.

The HOMO-LUMO profiles of PYZ in CTAB & SDS involves closely related MO profiles but with a different positioning in their respective molecular orbital diagrams (Figure 6a, 6b). This clearly indicates that the micellar-charge induced environmental modifications of PYZ invoke some noticeable variations in its MO diagram. This is probably the most apt reason owing to which the maximum emission wavelength of PYZ (excited at 381nm) is almost equal (~ 499 nm) in both ionic micellar media (CTAB & SDS). TX-100, being a neutral species does not efficiently alter the HOMO-LUMO distribution profile of PYZ (Figure 6c). The HOMO, LUMO and their corresponding energy gaps (ΔE) were assigned [Figure S3(a) & S3(b)] and calculated for each PYZ-micelle and PYZ-micelle-quencher systems (Table 3). It was observed that PYZ exhibits lower HOMO-LUMO energy gaps in both micellar media than that in bulk aqueous medium. In the HOMO-LUMO calculations of PYZ in fluorescence quenching studies, it was observed that for PYZ-SDS-CpCl the HOMO is predominantly delocalized over SDS and partially over CpCl i.e the HOMO has completely shifted from PYZ to the micelle-quencher network. The LUMO has predominantly delocalized only over the quencher CpCl thus making it facile for further electron accommodation (Figure 7a & 7b). This is absolutely a unique observation where the fluorophore, micelle and the quencher interact with each other in a unique way which is totally complementary to a general probe-micelle-quencher system. This unequivocally explains the actual cause for the anomalous enhancement in fluorescence intensity of PYZ in SDS, upon addition of quencher CpCl (Figure 8). Undoubtedly, this is very strong and justifiable evidence in support of our earlier assumption that PYZ-SDS-CpCl interact with each other in a very specific manner, which is totally uncommon for any probe-micelle-quencher system. As a result the PYZ emission intensity increased markedly in SDS micelles when added with quencher CpCl.

Figure 8: MO diagrams of PYZ* in SDS and SDS-CpCl media along with their corresponding energy values calculated by TD-DFT / B3LYP / 6-31G (d, p) method



In case of PYZ-TX-100-CpCl, both the HOMO and LUMO remains predominantly delocalized over the PYZ moiety, indicating that PYZ is still the active site for any further reaction (Figure 7c & 7d). Due to this reason CpCl was able to quench the

fluorescence of PYZ in TX-100 micellar media quite effectively. In fact fluorescence quenching of PYZ emission was maximum in case of PYZ-TX-100-CpCl system as observed from steady state fluorescence quenching studies. The high K_{sv} values of PYZ in this particular micellar media also supported the observation. In overall, the TD-DFT calculated results were able to account for the unique spectral behaviour of PYZ qualitatively to quite a reasonable extent. Certainly there remains a few aspects for improvement like a more accurate quantitative analysis with better precision and accuracy, but nevertheless, this TD-DFT/B3LYP/6-31G(d,p) analysis has substantially provided an unique and intriguing insight into the “micellar charge” specific photophysical behaviour of bio-active PYZ molecule, in its first singly excited state.

4. Conclusion:

The photophysical response of PYZ with ionic and nonionic micelles yielded distinctive and substantial results. PYZ emission was found to be more media dependent compared to absorption thus indicating its enhanced photo response in the excited state. The prominent *red shift* in the emission wavelength maxima of PYZ in ionic micelles arises from specific electrostatic interactions between PYZ and the ionic micelles. The emission maxima of PYZ in aqueous medium essentially originates due to a less coplanar structure of the PYZ molecule; whereas the *red-shifted* emission band (in CTAB & SDS) originates from a probe structure bearing a perpendicular conformation between the pyrazolyl and pyrazol rings linked by a double bond thereby rendering a certain degree of co-planarity to the PYZ molecule. In CTAB & SDS, the *pre-micellar red shift* in PYZ emission maxima at *surfactant concentration lower than its cmc*, occurs due to the formation of *pre-micellar aggregates* of the ionic surfactants in the experimental solutions. Under appropriate conditions PYZ is preferentially stabilized in the singly excited state owing to a greater dipole moment than that of its ground state precursor. The excited state conformational relaxation in PYZ is possible by bond rotation at a number of sites including the carbon-carbon bonds between the aromatic centers as well as the -CN bond in the aromatic ring. The steady state emission results were exploited to determine the binding efficiency of excited PYZ molecule with the micelles which revealed that the binding constant (K) of PYZ is greater with nonionic micelle TX-100 than that with the ionic micelles (CTAB and SDS) due to strong binding affinity between PYZ and the thick palisade layer of TX-100 micelles. Among the ionic ones, the binding constant of PYZ in SDS is considerably higher than that in CTAB by virtue of a stronger electrostatic interaction persisting between PYZ and SDS. The *electrostatic contribution* of PYZ decreases with *increasing hydrophobic character* of the ionic micelles which is reflected properly by the experimentally observed K values of PYZ in CTAB and SDS. Fluorescence quenching of PYZ by CpCl produced negligible quenching in CTAB in contrast to an efficient one in TX-100. However, in SDS, dramatic enhancement of PYZ emission was observed instead of normal quenching. It is predicted that the polar excited state of PYZ is highly stabilized by the co-operative effects of the negative charge of SDS and the positive charge of quencher CpCl leading to an overall increase in the emission sensitivity of the

molecule. Lifetime measurements hinted towards the possible existence of the proposed PYZ in multi-environmental media, as evident from the bi-exponential decay curve of PYZ in aqueous as well as in all micellar media. The short lifetime component of PYZ exhibit almost similar values in every medium which may be attributed to the presence of unbounded free probe in bulk aqueous solution. The long lifetime component PYZ, whose contribution is small (8%) in water, progressively increases in each micellar media indicating its predominance in a micellar micro-environment. A simple yet unique attempt was successfully adopted with an aim to interpret these experimentally observed spectral changes in terms of variation in the distributional behaviour of the frontier molecular orbital's (HOMO-LUMO) of PYZ; since MO's play a vital role in any electrostatic interaction. The theoretically calculated TD-DFT results promptly indicate that the variation of charge indeed caused noticeable changes in the HOMO and LUMO profiles of PYZ. The HOMO-LUMO energy gap calculations of PYZ in aqueous and micellar media confirms that the neutral form of PYZ is predominant in the ground state whereas the zwitterionic form gains stability in every micellar media owing to a *greater transition probability* in the excited state (*lower HOMO-LUMO energy gap*). The HOMO-LUMO calculations of PYZ-SDS-CpCl system provided useful insight regarding the actual cause for the anomalous fluorescence enhancement of PYZ in SDS upon addition of quencher CpCl. Summing up; this work explicitly demonstrates the “micellar charge” dependence on the modulated spectral behavior of PYZ. Since, surfaces and interfaces capable of repelling, attracting, and selectively detecting molecules have attracted attention for their important application in catalysis, coatings, sensors, and devices, including biologically implantable ones, the current results provide pertinent scope to comprehend the role and effect of “micellar charge” in modifying the spectroscopic response of other bio-active fluorescent probes. In view of the above mentioned facts and the wide spread use of pyrazoline derivatives in bio-medicinal fields, this selective “medium-charge specific” photophysical response of “PYZ” is undoubtedly an encouraging and prospective observation in the arena of contemporary research. Employing this micellar charge dependent emissive response of “PYZ” should provide adequate information to researchers for designing a new fluoro-sensing mode for ionic and neutral molecules within a variety of organized media and structured bio-assemblies.

Acknowledgement

Authors thank Prof. K.K. Mahalanabis and Dr. A. Mukherjee of Jadavpur University for their invaluable co-operation with the synthesis of the compound. Author A.S. thanks “CSIR, Govt. of India” for providing RA fellowship. Financial assistance from CSIR [01(2429) / 10 / EMR-II] is gratefully acknowledged.

Notes and References

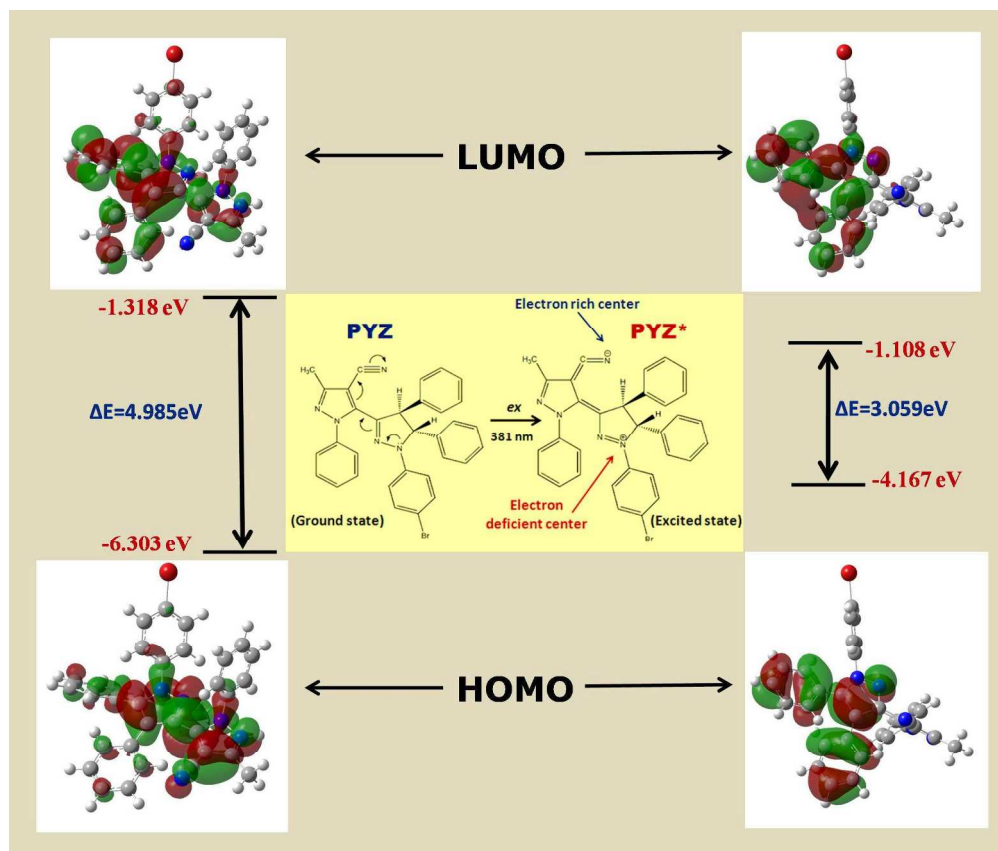
^a Department of Chemistry, Jadavpur University, Jadavpur, Kolkata-700032, India. Fax: 91(033) 24146584; Tel: 033 2414 6223; E-mail: sbjuchem@yahoo.com, scbhattacharyya@chemistry.jdvu.ac.in

^b Departamento de Química Física, Facultad de Ciencias y Tecnología Universidad del País Vasco-EHU Apartado 644, 48080-Bilbao, Spain

† Electronic Supplementary Information (ESI) available:

10 Normalized absorption spectrum of PYZ in different micellar environments; MO diagrams of PYZ in different micellar media along with their corresponding energy values.

- (1) H. Raghuraman and A. Chattopadhyay, *Eur Biophys J.* 2004, **33**, 611.
 15 (2) S. McLaughlin, *Annu. Rev. Biophys. Biophys. Chem.* 1989, **18**, 113.
 (3) Q. Zhang, N. R. Ko, J. K. Oh, *Chem. Commun.* 2012, **48**, 7542.
 (4) S. P. Wang, Y. T. Wang, *J. Controlled Release*, 2012, **159**, 312.
 (5) T. Sakthivel, A. T. Florence, *Drug Deliv. Technol.* 2003, **3**, 73.
 (6) K. Anwer, C. Meaney, G. Kao, N. Hussain, R. Shelvin, R. M. Earls, P. Leonard, A. Quezada, A. P. Roland, S. M. Sullivan, *Cancer Gene Therapy*, 2000, **7**, 1156.
 20 (7) A. Jahn, W. N. Vreeland, D. L. DeVoe, L. E. Locascio, M. Gaitan, *Langmuir*, 2007, **23**, 6289.
 (8) K. Holmberg, *Curr. Opin. Colloid Interface Sci.* 2003, **8**, 187.
 25 (9) K. Fuji, T. Morimoto, K. Tsutsumi, K. Kakiucki, *Angew. Chem., Int. Ed.* 2003, **42**, 2409.
 (10) T. Dwars, E. Paetzold, G. Oehme, *Angew. Chem., Int. Ed.* 2005, **44**, 7174.
 (11) H. Gröger, O. May, H. Hüskén, S. Georgeon, K. Drauz, K. Landfester, *Angew. Chem., Int. Ed.* 2006, **45**, 1645.
 30 (12) J. Li, Y. M. Zhang, D. F. Han, G. Q. Jia, J. B. Gao, L. Zhong, C. Li, *Green Chem.* 2008, **10**, 608.
 (13) F. Trentin, A. M. Chapman, A. Scarso, P. Sgarbossa, A. R. Michelin, G. Strukul, D. F. Wass, *Adv. Synth. Catal.* 2012, **354**, 1095.
 35 (14) L. Laville, C. Charnay, F. Lamaty, J. Martinez, E. Colacino, *Chem. Eur. J.* 2012, **18**, 760.
 (15) V. Rammurthy, (ed) *Photochemistry in organized and constrained media*. 1991, VCH, New York.
 (16) K. Kalyanasundram, *Photochemistry in microheterogeneous systems*. 1987, Academic, New York.
 40 (17) K. L. Mittal, B. Lindman, (eds) *Surfactants in solution*, Vol:1–3. 1994, Plenum, New York.
 (18) N. J. Turro, M. Gratzel, A. M. Braun, *Angew. Chem. Int. Ed. Engl.* 1980, **1**, 675.
 45 (19) J. Shobha, V. Srinivas, D. Balasubramanian, *J. Phys. Chem.* 1989, **93**, 17.
 (20) F. Grieser, C. J. Drummond, *J. Phys. Chem.* 1988, **92**, 5580.
 (21) J. R. Goodell, F. Puig-Basagoiti, B. M. Forshey, P.-Y. Shi, D. M. Ferguson, *J. Med. Chem.* 2006, **49**, 2127.
 50 (22) L. K. Ravindranath, K. Srikanth, M. Dastagiri Reddy, S. D. Ishrath Begum, *Heterocycl. Commun.* 2009, **15**, 443.
 (23) A. A. Farghaly, A. A. Bekhit, J. Y. Park, *Arch. Pharm. Pharm. Med. Chem.* 2000, **333**, 53.
 (24) E. Palaska, M. Aytemir, I. T. Uzbay, D. Erol, *Eur J. Med. Chem.* 2001, **36**, 539.
 55 (25) S. G. Kucukguzel, S. Rollas, *II Farmaco*, 2002, **57**, 583.
 (26) T.-S. Jeong, K. S. Kim, S.-J. An, K.-H. Cho, S. Lee, W. S. Lee, *Bioorg. Med. Chem. Lett.* 2004, **14**, 2715.
 (27) T. Nakagawa, M. Fujio, T. Ozawa, M. Minami, M. Satoh, *Behav. Brain Res.* 2005, **156**, 233.
 60 (28) S. Chatterjee, P. Banerjee, S. Pramanik, A. Mukherjee, K. K. Mahalanabis, S. C. Bhattacharya, *Chem. Phys. Lett.* 2007, **440**, 313.
 (29) S. Pramanik, P. Banerjee, A. Sarkar, A. Mukherjee, K. K. Mahalanabis, S. C. Bhattacharya, *Spectrochim. Acta: Part A*, 2008, **71**, 1327.
 65 (30) P. Banerjee, S. Pramanik, A. Sarkar, S. C. Bhattacharya, *J. Phys. Chem. B* 2008, **112**, 7211.
 (31) P. Banerjee, S. Pramanik, A. Sarkar, S. C. Bhattacharya, *J. Phys. Chem. B*, 2009, **113**, 11429.
 70 (32) A. Sarkar, T. K. Mandal, D. K. Rana, S. Dhar, S. Chall, S. C. Bhattacharya, *J. Lumin.* 2010, **130**, 2271.
 (33) A. Sarkar, S. C. Bhattacharya, *J. Lumin.* 2012, **132**, 2612.
 (34) A. Mukherjee, K. K. Mahalanabis, *Heterocycles*, 2009, **78**, 911.
 (35) W. Zhao, W. Bian, *J. Mol. Struct.: Theochem*, 2007, **818**, 43.
 75 (36) V. Barone, M. Cossi, and J. Tomasi, *J. Comp. Chem.* 1998, **19**, 404.
 (37) M. Almgren, F. Grieser, J. K. Thomas, *J. Am. Chem. Soc.* 1979, **101**, 279.
 (38) N. J. Turro, A. Yekta, *J. Am. Chem. Soc.* 1978, **100**, 5951.
 (39) G. Saroja, B. Ramachandram, S. Saha, A. Samanta, *J. Phys. Chem. B* 1999, **103**, 2906.
 80 (40) M. Kumbhakar, T. Goel, T. Mukherjee, H. Pal, *J. Phys. Chem. B*, 2004, **108**, 19246.
 (41) P. Hansson, M. Almgren, *J. Phys. Chem B*, 2000, **104**, 1137.
 (42) G. Komaromy-Hiller, N. Calkins, R. von Wandruszka, *Langmuir*, 1996, **12**, 916.
 85 (43) J. R. Lakowicz, *Principles of Fluorescence Spectroscopy*; 1999, Kluwer-Plenum Press: New York.
 (44) H. Y. Song, S. W. Oh, S. D. Moon, Y. S. Kang, *J. Colloid. Int. Sci.* 2007, **314**, 683.
 90 (45) N. A. Smirnova, B. Murch, I. B. Pukinsky, T. G. Churjusova, M. V. Alexeeva, *Langmuir*, 2002, **18**, 3446.
 (46) S. W. Oh, S. D. Moon, D. K. Lee, D. J. Lee and Y. S. A. Kang, *Bull. Korean Chem. Soc.* 2004, **25**, 280.
 (47) F. V. Bright, C. A. Munson, *Anal. Chim. Acta.* 2003, **500**, 71.
 95 (48) M. Shannigrahi, S. Bagchi, *J. Photochem. Photobiol. A: Chem.* 2004, **168**, 133.
 (49) S. Chen and J. Duhamel, *Langmuir*, 2013, **29**(9):2821.
 (50) A. Samanta, B. K. Paul & N. Guchhait, *J. Fluorescence*, 2012, **22**, 289.
 100 (51) C. F. A. Gomez-Duran, I. Garcia-Moreno, A. Costela, V. Martin, R. Sastre, Jo. Banuelos, F. Lopez Arbeloa, I. Lopez Arbeloa and E. Pena-Cabrera, *Chem. Comm.* 2010, **46**, 5103.
 (52) J. Banuelos, I. J. Arroyo-Cordoba, I. Valois-Escamilla, A. Alvarez-Hernandez, E. Pena-Cabrera, R. Hu, B. Z. Tang, I. Esnal, V. Martinez and I. Lopez Arbeloa, *RSC Adv*, 2011, **1**, 677.
 105 (53) C.-G. Zhan, J. A. Nichols and D. Dixon, *J. Phys. Chem. A*, 2003, **107**, 4184.
 (54) G. Zhang and C. Musgrave, *J. Phys. Chem. A*, 2007, **111**, 1554.
 (55) J. Banuelos, F. Lopez Arbeloa, V. Martinez, M. Liras, A. Costela, I. G. Morenoc and I. Lopez Arbeloa, *Phys. Chem. Chem. Phys.* 2004, **6**, 4247.
 110 (56) J. Banuelos Prieto, F. Lopez Arbeloa, V. M. Martinez, T. Arbeloa Lopez and I. Lopez Arbeloa, *Phys. Chem. Chem. Phys.* 2011, **13**, 3437.
 115 (57) I. Kaur, W. Jia, R. P. Kopreski, S. Selvarasah, M. R. Dokmeci, C. Pramanik, N. E. McGruer and G. P. Miller, *J. Am. Chem. Soc.* 2008, **130**, 16274.
 (58) V. Bèreau, C. Duhayon, A. Sournia-Saquet and J.-P. Sutter, *Inorg. Chem.* 2012, **51**, 1309.
 120 (59) B.-Gi. Kim, X. Ma, C. Chen, Y. Ie, E. W. Coir, H. Hashemi, Y. Aso, P. F. Green, J. Kieffer, J. Kim, *Adv. Funct. Mater.* 2013, **23**, 439.
 (60) H. Zhang, X. Wan, X. Xue, Y. Li, A. Yu, Y. Chen, *Eur. J. Org. Chem.* 2010, **9**, 1681.
 125 **Gaussian-09^{HR} developed by: Gaussian, Inc., Wallingford CT, 2009.
M. J. Frisch, G. W. Trucks, H. B. Schlegel, G. E. Scuseria, M. A. Robb, J. R. Cheeseman, G. Scalmani, V. Barone, B. Mennucci, G. A. Petersson, H. Nakatsuji, M. Caricato, X. Li, H. P. Hratchian, A. F. Izmaylov, J. Bloino, G. Zheng, J. L. Sonnenberg, M. Hada, M. Ehara, K. Toyota, R. Fukuda, J. Hasegawa, M. Ishida, T. Nakajima, Y. Honda, O. Kitao, H. Nakai, T. Vreven, J. A. Montgomery, Jr., J. E. Peralta, F. Ogliaro, M. Bearpark, J. J. Heyd, E. Brothers, K. N. Kudin, V. N. Staroverov, R. Kobayashi, J. Normand, K. Raghavachari, A. Rendell, J. C. Burant, S. S. Iyengar, J. Tomasi, M. Cossi, N. Rega, J. M. Millam, M. Klene, J. E. Knox, J. B. Cross, V. Bakken, C. Adamo, J. Jaramillo, R. Gomperts, R. E. Stratmann, O. Yazyev, A. J. Austin, R. Cammi, C. Pomelli, J. W. Ochterski, R. L. Martin, K. Morokuma, V. G. Zakrzewski, G. A. Voth, P. Salvador, J. J. Dannenberg, S. Dapprich, A. D. Daniels, Ö. Farkas, J. B. Foresman, J. V. Ortiz, J. Cioslowski, and D. J. Fox,



HOMO-LUMO distribution of PYZ in its ground and first singly excited state
688x582mm (96 x 96 DPI)